J Appl Electrochem (2013) 43:773–782
DOI 10.1007/s10800-013-0573-y

ORIGINAL PAPER

Graphite oxide/polypyrrole composite electrodes for achieving high energy density supercapacitors

Arvinder Singh · Amreesh Chandra

Received: 26 April 2013 / Accepted: 25 June 2013 / Published online: 9 July 2013

Abstract Fabrication and characterization of high energy density supercapacitor based on graphite oxide/polypyrrole (GO/PPy) composites is reported. Improvement in charge storage has been obtained by exfoliation of graphite oxide sheets via intercalation of polypyrrole. The formation of composite has been shown by the analysis of X-ray diffraction, Raman spectroscopy, X-ray photoelectron spectroscopy, and Fourier transfer of infrared spectroscopy data. Scanning electron and transmission electron microscopy clearly show sheet-like layered structure of graphite oxide surrounded by polypyrrole. Supercapacitors fabricated using this composite system result in a reduced equivalent series resistance value $\sim 1.85\ \Omega$. Such low value can be attributed to the intercalation of conducting polypyrrole into the graphite sheets. A specific capacitance of $\sim 181\ F\ g^{-1}$ in 1 M Na_2SO_4 aqueous electrolyte with a corresponding specific energy density of $\sim 56.5\ Wh\ kg^{-1}$ could be achieved. These values make GO-based materials suitable for their use as electrodes in high performance supercapacitors.

Keywords Graphite oxide · Conducting polymer · Composites · Supercapacitors

Electronic supplementary material The online version of this article (doi:10.1007/s10800-013-0573-y) contains supplementary material, which is available to authorized users.

A. Singh (✉) · A. Chandra
Department of Physics and Meteorology, Indian Institute of Technology Kharagpur, Kharagpur 721302, West Bengal, India
e-mail: asphy.2008@gmail.com

A. Chandra
e-mail: achandra@phy.iitkgp.ernet.in

1 Introduction

Majority of our energy requirements are presently being met by technologies based on conventional energy sources such as fossil fuel, hydro, gas, and nuclear [1]. Excessive use of such sources has been the major contributor to climate change [2]. Consequently, there is increasing demand to combine conventional and renewable energy sources to achieve environmentally friendly, readily available, and socially acceptable energy technologies. Among the renewable energy sources being explored: solar, wind, and bio-based technologies have been the most successful. However, the intrinsic "*intermittent*" nature of renewable sources restricts their rapid growth and large scale implementation. For example—solar-based production units perform best on a clear day, or wind energy is mainly available during certain time depending upon the geographic location [3]. Consequently, a sustainable renewable energy source needs to be supported by an electrical energy storage system (EESS). An EESS helps to have reduced fluctuations/spikes, continuity of supply, and high efficiency of grid during both peak and off-peak periods. An ideal EESS system would be the one that can supply high burst or pulsed power, has high energy density and is cost effective. Out of modern day EESSs that deliver high power while maintaining moderate energy density values, electrochemical capacitors (ultracapacitors or supercapacitors) are the most promising [4]. On the other hand, Li-ion batteries are used at places where high energy and moderate power density is required.

Supercapacitors (SCs) are high power electrochemical capacitors with fast charge/discharge rates, long cycle life, low cost, and minimal maintenance [5, 6]. This makes them ideal candidates for use in power supplies, portable electronic devices, hybrid electric vehicles, power

invertors, and electrochemical actuators [7]. SCs store charges either electro-statically at each electrode/electrolyte interface (electrochemical double layer capacitors; EDLCs) or using fast and reversible redox reactions (pseudocapacitors). However, lower specific energy densities in comparison to batteries limit their range of applications [8]. To bring incremental change in SCs performance, use of new materials that allow high charge storage capacity is an accepted way forward. Desired parameters for such new electrode materials are: high surface area with tunable porosity, appreciable electronic conductivity, improved chemical and thermal stability, high purity, and low toxicity [9].

Most commercially available SCs use various forms of carbon as electrode material [10, 11]. This limits maximum achievable specific capacitance, since charge accumulation gets restricted to the carbon surface only. To overcome this limitation, few redox materials have been proposed [12–16]. But such devices continue to have short cycle life and low power density. Recently, graphene-based materials have shown promising characteristics for developing high performance supercapacitors [17, 18]. However, restacking of graphene sheets during synthesis has a significant detrimental effect on the performance of SCs. Further, high cost of graphene and its reproducibility remain a challenge. Therefore, a material that possesses exfoliated structure similar to graphene for easy charge intercalation and is free of stacking problem would be an interesting alternative.

Recently, exfoliated graphite oxide (GO) has been reported as the electrode material for supercapacitors [19, 20]. Exfoliated structures generally have more edge plane sites along with high surface area. This allows faster charge transfer and induces higher storage capacity. Exfoliated GO has layered structure with epoxide, carbonyl, and hydroxyl functional groups occupying interlayer space. These GO sheets with hydrophilic nature can provide high surface area backbone to hydrated ions of the aqueous electrolyte for adsorption. This leads to the double layer capacitance at each electrode. However, the presence of these functional groups results in reduced electrical conductivity. One logical and convenient option to overcome this limitation would be the insertion of electrically conducting polymers between the GO sheets. This would promote electrolyte ion transportation as well as brings acceptable electrical conductivity and mechanical strength [19, 20].

Among the conducting polymers, polypyrrole (PPy) is recognized for its easy synthesis, high electrical conductivity, fast charging–discharging ability, and environmental compatibility [21]. In this work, we report the synthesis and use of exfoliated GO with intercalated PPy rings. Intercalated PPy ensures a better accessibility of electrolyte ions into the GO sheets, improved charge conduction, and makes possible the fabrication of high performance SCs. A scheme depicting the structure of the proposed electrode material is shown in Fig. 1. In the fabricated SCs, a maximum specific capacitance of $\sim$181 F g^{-1} and energy density of $\sim$56.5 Wh kg^{-1} could be obtained at a scan rate of 10 mV s^{-1} using 1 M Na_2SO_4 aqueous electrolyte. The corresponding specific power density of $\sim$1,356 W kg^{-1} is obtained, which reaches to a value of $\sim$11,237 W kg^{-1} at a scan rate of 200 mV s^{-1} with a reduced energy density of $\sim$23.4 Wh kg^{-1}. These energy and power density values are higher than most of the previously reported values for carbon-based supercapacitors [22–24]. The work presented here clearly suggests that GO/conducting polymer composite would be an interesting material for obtaining a high energy density in SCs.

2 Experimental

2.1 Materials used

Graphite fine powder (particle size 50 μm, purity 99 %) was purchased from Loba Chemie Pvt. Ltd. (India). Sulfuric acid (98 %), hydrochloric acid (35 %), hydrogen peroxide solution GR (30 %), methanol, ferric chloride anhydrous (96 %), and potassium permanganate (98.5 %) were purchased from Merck Specialities Pvt. Ltd. (India). Pyrrole monomer extra pure (M.W. 67.09, 98 %) was purchased from Sisco Research Laboratories Pvt. Ltd. (India). All chemicals were used as purchased without any further purification.

2.2 GO and PPy synthesis

Graphite oxide was synthesized by following the modified Hummer's method [25]. PPy was synthesized by dissolving pyrrole (0.2 mol) in 50 mL of (1:1) methanol/de-ionized water (DI) solution. On addition of 50 mL ferric chloride (0.1 M) solution as initiator, polymerization was started immediately. The solution was kept stirring continuously

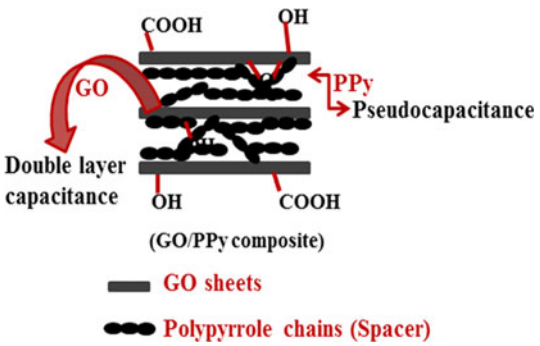

Fig. 1 A schematic depicting the structure of the proposed electrode material

for 24 h at room temperature. PPy was obtained by filtration, washing several times with DI/methanol solution and finally vacuum drying at 60 °C for 24 h.

2.3 GO/PPy composite synthesis

To prepare GO/PPy composites, synthesized GO (0.2 g) was dispersed in 20 mL of DI water using an ultrasonication bath to get a homogeneous solution. Then, a solution of PPy dispersed in dimethylformamide (DMF; 80 mL) was mixed to the GO dispersion and the mixed solution was once again ultrasonicated for 30 min. For ensuring homogeneous dispersion, the solution was then stirred at room temperature for 12 h. Consequently, a few drops of HCl were added to re-stack GO sheets having trapped PPy between them. Finally, the solution was heated at 60 °C, centrifuged and vacuum dried at 70 °C for 12 h. The composite formation was confirmed using XRD, Raman, XPS, and FTIR, while the morphological investigation was carried out using electron microscopy data.

2.4 Material characterization

XRD analysis was carried out using an X'pert Pro diffractometer operated at 1.6 kW (i.e., 40 kV and 40 mA) in 2θ range 5°–40° with Cu K_α as the incident radiation. Fourier transfer infrared spectroscopy (FTIR) spectra were obtained at room temperature using Spectrum BX FTIR (Perkin Elmer version 5.3). X-ray photoelectron spectroscopy (XPS) data were collected using the PHI 5000VERSA Probe II X-ray photoelectron spectrometer with Al K_α X-ray as an excitation wavelength. Raman spectroscopic data was collected on MODEL T64000 spectrometer with laser wavelength 488 nm. For morphological investigations, scanning electron microscopy (SEM CARL ZEISS SUPRA 40) and transmission electron microscopy (TEM-FEI-TECHNAI G220S-Twin operated at 200 kV) were performed. Four probe resistivity measurements were performed using Keithley 6221 and Keithley Multimeter 2000.

2.5 Supercapacitor fabrication and characterization

For the fabrication of GO/PPy electrodes, 85 wt% synthesized GO/PPy material, 10 wt% acetylene black, and 5 wt% Poly(vinylidene fluoride-co-hexafluoropropene) (PVDF-HFP) were mixed in acetone till a thick slurry which was obtained. This slurry was then brush coated on a graphite sheet. Electrodes (each with area ~ 1 cm^2) were fabricated by cutting coated graphite sheet followed by vacuum drying at 100 °C for 24 h. A glass fiber paper presoaked in 1 M Na_2SO_4 aqueous solution was sandwiched between two fabricated electrodes to construct symmetric supercapacitor device. Electrochemical measurements of the fabricated supercapacitor were carried out using an electrochemical analyzer (model 608C, CH Instruments) and the charge–discharge measurement unit (model BT2000, Arbin Instruments, College Station, TX).

3 Results and discussion

3.1 X-ray diffraction analysis

X-ray diffraction method is widely used for characterization of structured materials. It is known that interlayer spacing of GO sheets depends upon degree of oxidation, i.e., attached functional groups and number of intercalated water molecules during growth. Variation (addition/removal) of these functional groups will change the interplanar, i.e., d-spacing values. Typical XRD patterns of synthesized GO and GO/PPy composites are shown in Fig. 2. The diffraction maxima at $2\theta \approx 11.24°$ with an inter-planar spacing $d = 0.79$ nm is observed, which corresponds to (002) plane of GO, (as shown in the inset of Fig. 2). For the case of the composite system, (002) reflection peak shifts to $2\theta \approx 12.84°$, which corresponds to the inter-planar distance $d = 0.70$ nm. This reduced d-value seems to contradict the claim that polymer has penetrated the GO interlayer spacing. But this is not true. The result is consistent with the claim as it clearly suggests that polymer replaces the water attached to the GO layers. This feature has been reported by earlier workers [26]. Intensity of this peak also gets reduced which suggests exfoliation of GO sheets. The presence of PPy in GO/PPy composite is visible from a characteristic broad peak of PPy appearing at $2\theta \approx 29.5°$, as zoomed in inset to Fig. 2.

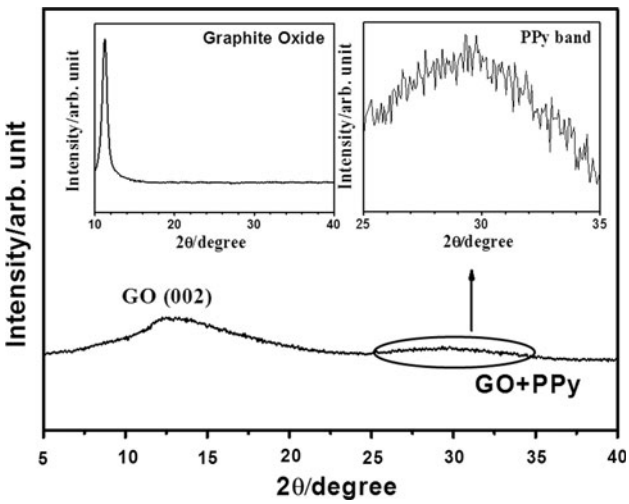

Fig. 2 Typical X-ray diffraction pattern of graphite oxide (GO)/polypyrrole (PPy) composites and GO (given as *inset*)

3.2 Raman analysis

Raman spectroscopy is frequently used for characterization of carbon materials, since conjugated as well as C=C bond give high Raman intensities [27]. Raman spectra of the prepared GO and GO/PPy composites are shown in Fig. 3. For the GO system, the G-band appears due to in-plane sp^2 carbons, while the D-band is associated with presence of defects (edges, functional groups, etc.) in GO structure [28]. In the synthesized GO, characteristic D and G bands were observed at $\sim$1,347 and $\sim$1,590 cm^{-1}, respectively, with an intensity ratio $I_D/I_G = 0.79$, as shown in inset to Fig. 3. After PPy intercalation, these D- and G-bands shift to $\sim$1,360 and $\sim$1,578 cm^{-1} with a small increase in the intensity ratio $I_D/I_G = 0.82$ (see Fig. 3). This increase in intensity ratio can be attributed to the creation of more defects in GO sheets during PPy intercalation. Two small peaks appearing at 868 and 1,047 cm^{-1} in GO/PPy composites are the characteristic peaks of PPy.

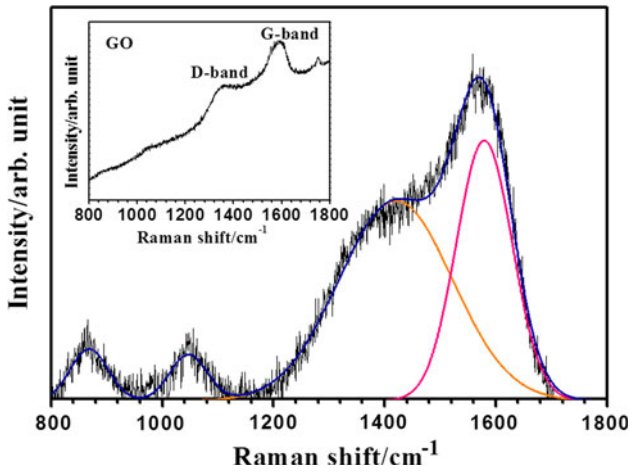

Fig. 3 Raman spectra of graphite oxide/polypyrrole composite. *Inset* to figure depicts the Raman spectra for pure graphite oxide (GO)

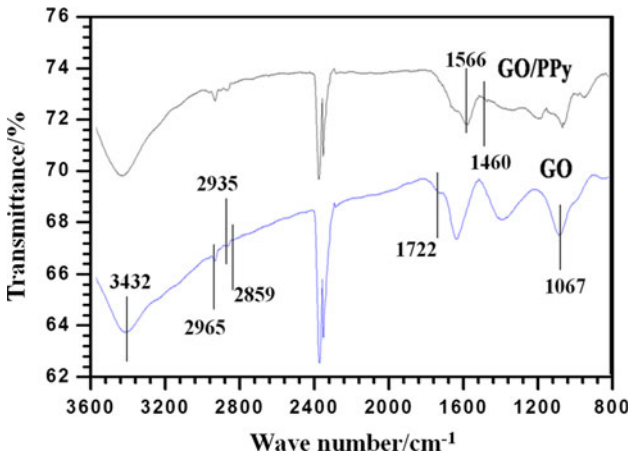

Fig. 4 FTIR spectrum of graphite oxide (GO) and GO/polypyrrole composite

3.3 FTIR analysis

The claim made earlier regarding change in surface due to the intercalation of PPy could be confirmed using FTIR spectra. The observed FTIR spectra of GO and GO/PPy are shown in Fig. 4. The peak at 3,432 cm^{-1} has been attributed to O–H bond stretching in water molecules and hydroxyl group of GO [29]. Origin of the peak at $\sim$2,965 cm^{-1} lies in the asymmetric stretching of C–H bond in $–CH_3$, while peaks at 2,935 and 2,859 cm^{-1} originate from asymmetric stretching and symmetric vibrations of C–H bond in $–CH_2$, respectively. The peak observed at 1,067 cm^{-1} is the characteristic peak of epoxide group; that shifts to 1,053 cm^{-1} in the composite system due to hydrogen bonding and π–π interaction between PPy and GO. The peak at $\sim$1,722 cm^{-1} is a consequence of carbonyl C=O stretching. Similarly, peaks at 1,566 and 1,460 cm^{-1} observed in GO/PPy spectra are due to C=C backbone stretching and C–N stretching vibration present in PPy ring, respectively. Intensity of these two peaks is small, since wt% of PPy in the GO/PPy is less; as evident from Table 1. FTIR results clearly show that the nature of characteristic peaks of individual components does not change. Moreover, there is no appearance of new peak or disappearance of existing peaks. This further confirms successful synthesis of GO/PPy composite.

3.4 Morphological investigations

SEM micrographs of the GO and GO/PPy show that pure GO exhibits flake like morphology, while in the GO/PPy, GO sheets are surrounded with PPy (Fig. 1, Online Resource 1). Re-stacking of GO sheets gets suppressed due to the PPy intercalation as observed from SEM monograph, which leads to random orientation of the GO sheets. Similar conclusions were drawn earlier based on XRD and Raman results. TEM micrographs of synthesized GO and GO/PPy composite and their selected area diffraction pattern (SEAD) are shown in Fig. 5a–c. GO sheets exhibit flake-like morphology, as shown in Fig. 5a, while hexagonal arrangement of six carbon atoms is observed in SEAD of GO, as depicted in the inset to Fig. 5a. Intercalation of

Table 1 Elemental composition of GO/PPy composite

Element	wt%	at.%
C	66.20	71.38
N	11.02	10.19
O	22.78	18.44

the PPy into GO sheets is confirmed from TEM image of GO/PPy, as shown in Fig. 5b. Regular arrangement of carbon atoms, as observed in SAED pattern of GO disappears in the SAED pattern of the GO/PPy due to the presence of amorphous PPy rings, as evident from inset to Fig. 5b. This further confirms the intercalation of PPy into GO sheets. An energy dispersive spectrum (EDS) of the GO/PPy was also recorded during TEM measurement, which is shown in Fig. 5c. All the peaks in the EDS of GO/PPy could be indexed to C, O, and N atoms, and composition of elements in wt% is shown in Table 1.

3.5 XPS study

The XPS spectra were also obtained for investigating the nature of bonding among elements present in GO and GO/PPy composite. Typical XPS spectrum is shown in Fig. 6. In the GO, carbon 1s and oxygen 1s peaks are observed at 283.17 and 530.42 eV, respectively, which again reappear at approximately same position in the GO/PPy composite. This shows that there is no chemical bonding between in-plane GO sheets and PPy rings. These results are in good agreement with previous reports [30]. In amine or pyrrolium nitrogen-based materials, which possess –NH structure, N 1s peak usually appears at binding energy of ~400 eV [30]. The presence of N 1s peak in the GO/PPy at 398.15 eV, which was absent in GO, again indicates the presence of PPy in the GO/PPy composite.

3.6 Four probe resistivity measurement

To investigate the improvement in electronic conductivity of GO after PPy intercalation, four probe resistivity measurements were carried out. Following equations were used to measure four probe resistivity of the GO and GO/PPy composite:

$$\text{Resistivity } \rho(\Omega\,\text{cm}) = (\pi t/\ln 2) \times (V/I)$$

and

$$\text{Conductivity } \sigma(\text{S/cm}) = 1/\rho$$

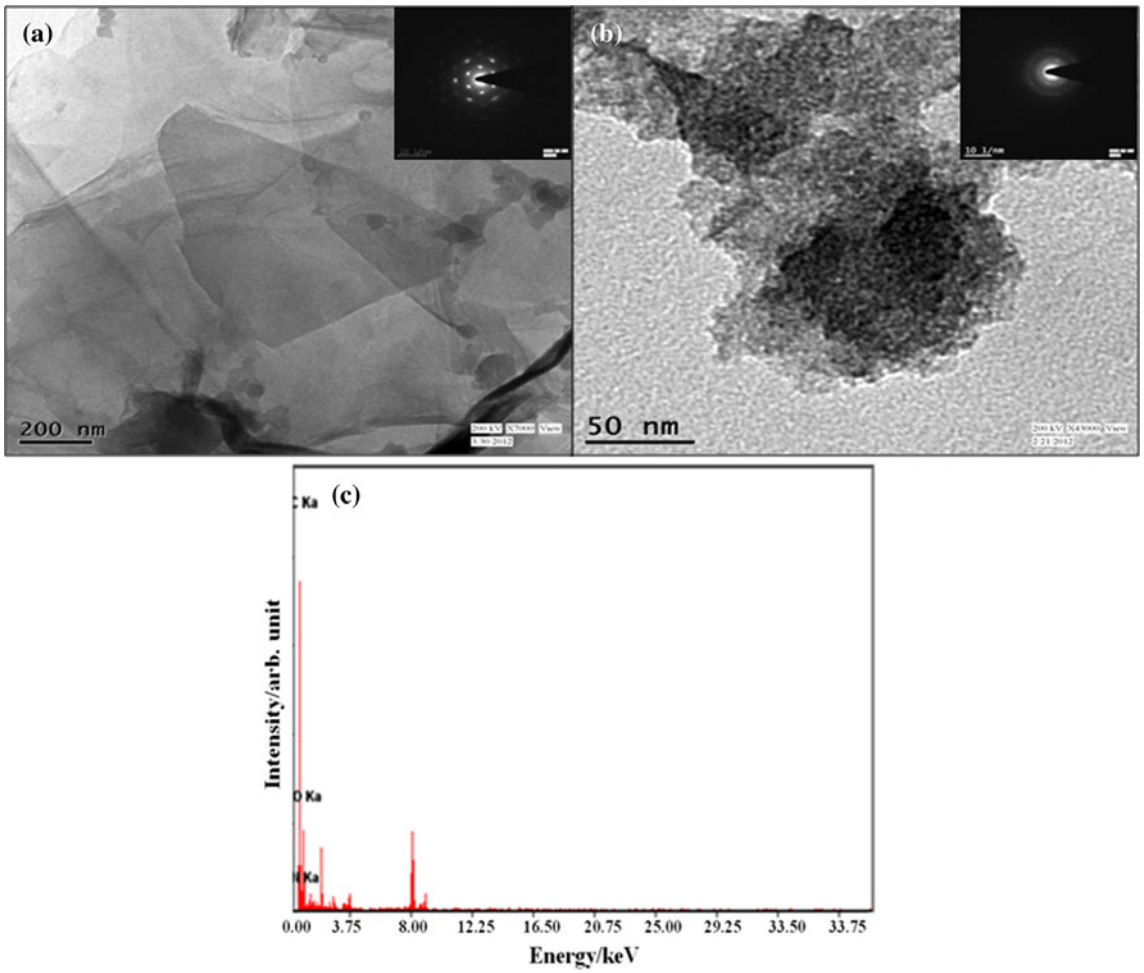

Fig. 5 **a** TEM image of GO and its SEAD pattern (given as *inset*), **b** TEM image of graphite oxide/polypyrrole composite and its SEAD pattern (given as *inset*), and **c** EDS spectra for GO/PPy composite

where t = thickness of the sample, V = measured voltage, and I = source current. Conductivity (σ) of GO was found $\sim 1.3 \times 10^{-5}$ S cm^{-1} whereas for GO/PPy, considerable improvement in the conductivity was measures with $\sigma \sim 1.7$ S cm^{-1}. Therefore, it can be confidently claimed that GO/PPy composite has reasonable conductivity, which makes them acceptable as electrode material for supercapacitors.

3.7 Electrochemical impedance spectroscopy (EIS)

As mentioned earlier, the GO/PPy composite system has capacity to allow higher intercalation of ions and facilitates efficient utilization of surface area related chemistry. Fabrication of SC using the composite system as electrode has been discussed in the Sect. 2. Electrochemical performance of such fabricated supercapacitor was determined with two electrode system by performing electrochemical impedance spectroscopy (EIS), cyclic voltammetry (CV), and galvanostatic charge–discharge measurements.

EIS is a well-known technique for evaluation of frequency response and equivalent series resistance (ESR) of supercapacitor device. A complex Nyquist plot for fabricated supercapacitor using GO/PPy composite is shown in Fig. 7. The ESR value, as evaluated by X-intercept of Nyquist plot, was $\sim 1.85\ \Omega$ for the present case (see inset to Fig. 7). In the Nyquist plot, one small semicircle in the high frequency region (46–1 kHz) indicates toward lower charge transfer resistance at electrode/electrolyte interface. The diameter of this semicircle represents magnitude of resistance for both ionic and electronic charge transfer between electrode material and electrolyte. Small charge transfer resistance occurs as PPy assisted exfoliated GO sheets facilitate ion transport via segmental motion and brings improvement to the conductivity of the composite material. This small resistance value in turn gives rise to high power density. At the lower frequency, SC shows good capacitive behavior since it possesses a vertical line almost parallel to imaginary axis.

3.8 Cyclic voltammetry analysis

Cyclic voltammetry (CV) curves of GO and GO/PPy composites based SCs obtained with two electrode assembly at different scan rates ranging from 0 to 1.5 V in 1 M Na_2SO_4 aqueous electrolyte are depicted in Fig. 8a, b. Aqueous Na_2SO_4 electrolyte was chosen for the present study, since it provides wider electrochemical voltage window, which is essential for achieving high energy density [31]. The GO based SC, at each scan rate, possesses irregular shaped CV curves due to presence of various functional groups, which can give rise to pseudocapacitance, as shown in Fig. 8a. However, the GO/PPy based SC shows roughly rectangular-shaped CV curves at each scan rate with higher current, which is a signature of much improved electrode (see Fig. 8b). The presence of functional groups on GO sheets and polypyrrole in the GO/PPy composite can store charge using following equations:

$$> C{=}O + e^- \Leftrightarrow > C - O^-$$

$$PPy \rightarrow PPy^{n+}(A^-)_n + ne^-$$

$$PPy + ne^- \rightarrow (C^+)_n PPy^{n-}$$

where A^- and C^+ are electrolyte anion and cation, respectively. Also, these CV curves are more horizontal in comparison to GO based SC, which confirms small contact resistance effect. Specific capacitance of fabricated SC was calculated from CV curves using following relation:

$$C = I/mS$$

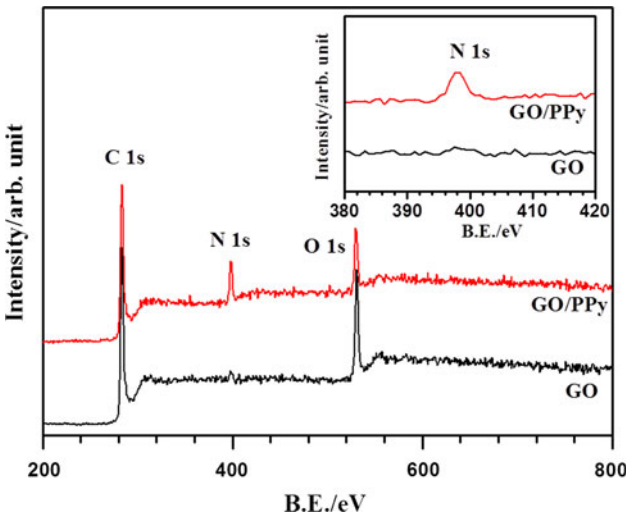

Fig. 6 X-ray photo electron spectroscopy (XPS) spectra of graphite oxide and graphite oxide/polypyrrole composite

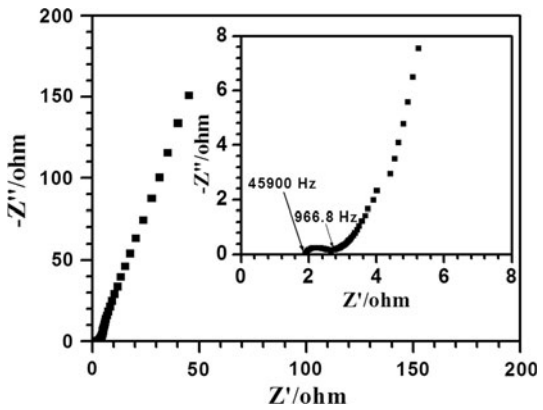

Fig. 7 Nyquist plot for graphite oxide/polypyrrole based supercapacitor (SC) between 100 kHz and 0.01 Hz in 1 M Na_2SO_4 aqueous electrolyte

where I is the average current, m is the mass of active materials (for both GO and GO/PPy composite in the present case, total mass is 2.2 mg for both electrodes excluding binder and for each electrode m is 1.1 mg), and S is the scan rate. A maximum specific capacitance of $\sim$181 F g^{-1} was obtained at a scan rate of 10 mV s^{-1}. Corresponding energy density and power density values were estimated using the following equations:

$$E = \frac{1}{2}CV^2; \quad P = E/t$$

where C is the specific capacitance in F g^{-1} and V is the applied initial voltage (here 1.5 V). The maximum energy density of $\sim$56.5 Wh kg^{-1} could be obtained, which corresponds to a specific power density of $\sim$1,356 W kg^{-1}. The effect of scan rate on specific capacitance for GO/PPy-based SC is shown in Fig. 9. The decrease of capacitance with increasing scan rate in CV curves can be explained to the fact that, at a higher scan rate, charge diffusion is not able to follow the variation in electric field, and thus returns small capacitance values and high power density. The SC retains corresponding energy density of $\sim$23.4 Wh kg^{-1} at a scan rate 200 mV s^{-1} while power density reaches to $\sim$11,237 W kg^{-1}. This shows good rate capability of fabricated SC. Using these results, few inferences regarding the performance of SC can be drawn viz., (a) intercalation of polymer facilitates diffusion of electrolyte ions into GO sheets as well as provides conducting contact between GO/PPy and electrolyte, and thus gives rise to fast rate charge transfer and (b) overall capacitance is a summation of contribution from pseudocapacitance and double layer capacitances (this is also elucidated from non-linear behavior of charge–discharge curves as discussed later). Cyclic stability is an important parameter for applicability of SC. In Fig. 10a, CV curves at different cycle no. (1st, 20, 40, 60, 80, 100, 200, 300, 400, 500, 600, 700, 800, 900, and 1000th) for GO/PPy based SC

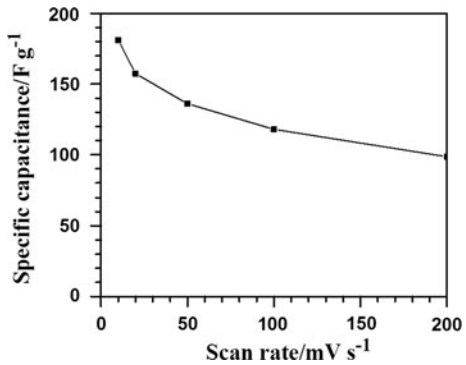

Fig. 9 Effect of scan rate on specific capacitance for GO/PPy-based SC

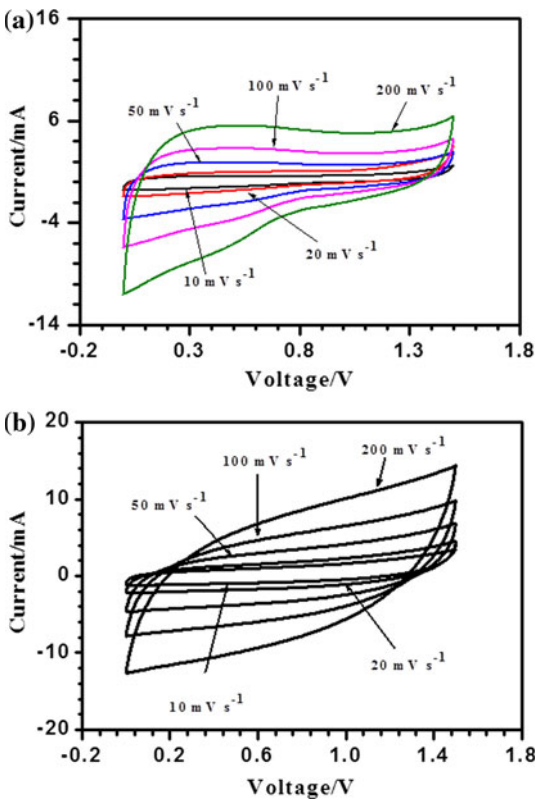

Fig. 8 Cyclic voltammetry (CV) curves of SC fabricated using **a** graphite oxide and **b** graphite oxide/polypyrrole composite between 0 and 1.5 V at different scan rates in 1 M Na_2SO_4 electrolyte

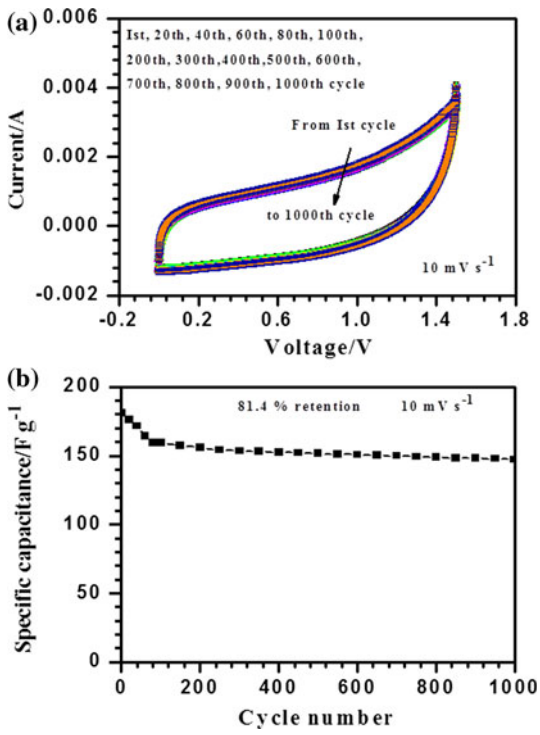

Fig. 10 **a** CV curves of GO/PPy-based SC for different cycle no. at a scan rate of 10 mV s^{-1}, and **b** specific capacitance variation with cycle no. for GO/PPy-based SC at 10 mV s^{-1} scan rates

at 10 mV s^{-1} scan rate are shown. Specific capacitance variation with cycle no. is also shown in Fig. 10b. The GO/PPy based SC retains ~81.4 % of its initial capacitance after 1000 cycles, which shows its suitability in various applications.

3.9 Galvanostatic charge–discharge

Galvanostatic charge–discharge measurement is a powerful tool for reliable characterization of supercapacitor devices. Galvanostatic discharge curves for the present device were recorded at different current densities of 1, 2, 5 mA cm^{-2} between 0 to 1.5 V and are shown in Fig. 11. The specific capacitance of supercapacitor was calculated using the following relation:

$$C(\mathrm{F/g}) = Idt/mdV$$

where I is the current density, dt is the discharging time, dV is the discharging voltage range, and m is the mass of active materials. Specific capacitance, energy density, and power density values are comparable to those calculated using CV data. The non-linear behavior of charge–discharge curves indicates contribution of pseudocapacitance in overall capacitance, which could be due to the PPy and/or various functionalities of the GO sheets. Wider charging/discharging voltage range and a lower ESR value allowed supercapacitor to achieve such high power density. These results are far superior than carbon-based supercapacitor, as discussed in the next section [32–34]. These results show applicability of GO/PPy based supercapacitors in wide range applications such as portable electronic devices, back-up supply and electric hybrid vehicles.

4 Comparison with previous studies

There are quite a few reports on carbon based materials in SCs, where electrochemical performance of carbon materials (graphene, multiwall carbon nanotubes, etc.) and their composite systems with PPy [32, 34–38]. As it is well established fact that, for applicability in various applications, SC must store high energy and have ability to deliver energy at fast rate. However, in all the above mentioned reports, either energy density or power density is dominating, as shown in Fig. 12. This clearly suggests that in these SCs, either carbon or polymer play the key role for charge storage while in our case, both GO and PPy are participating in charge storage, since specific capacitance estimated show double layer as well as pseudocapacitive contributions. We report the maximum energy density of ~56.5 Wh kg^{-1}, while the maximum power density of ~11,236 W kg^{-1}. Also, our GO/PPy composite exhibits excellent stability over wide voltage window with

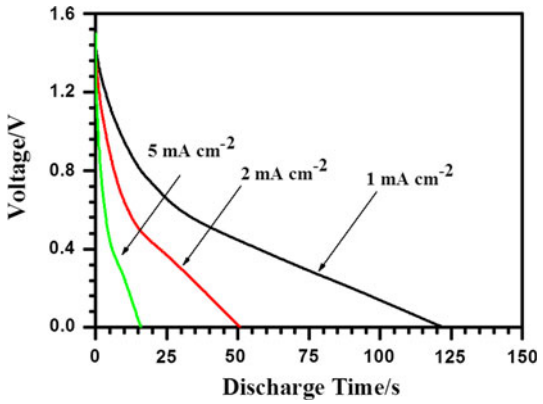

Fig. 11 Discharge curves of graphite oxide/polypyrrole based SC in the range of 0–1.5 V at various current densities in 1 M Na_2SO_4 electrolyte

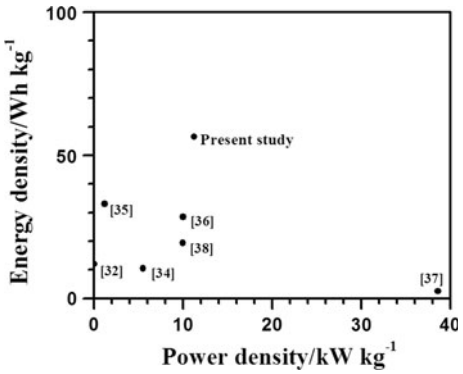

Fig. 12 Comparison of supercapacitor performance with previously reports

~81.4 % retention after 1,000 cycles. These energy and power density values make GO/PPy-based SC superior for various applications.

5 Conclusions

In this work, importance of exfoliated GO sheets with intercalated conducting polymer has been presented. The polymer not only helps to improve the conductivity of the system, but also acts like fillers, which lead to exfoliation of GO sheets. Such open structures are found to be extremely useful for application in supercapacitors. The SCs fabricated using GO/PPy composite system exhibited maximum energy density of ~56.5 Wh kg^{-1}, and maximum specific power density of ~11,236 W kg^{-1} in 1 M Na_2SO_4 aqueous electrolyte. These results are better than most of carbon based SCs. Further, these GO/polymer composites are low cost materials in comparison to graphene based materials, since there is no need for further reduction or purification and also, reproducible on a large

scale. These materials thus become extremely competitive to other well-known carbonaceous materials for supercapacitor applications.

Acknowledgments Arvinder Singh would like to thank CSIR (India) for the award of Junior Research Fellowship. Authors also acknowledge the FIST program of DST (India) for sanctioning funds for XPS instrument. We also would like to thank Prof. S. A. Hashmi, Department of Physics and Astrophysics, University of Delhi, Delhi for providing facilities to perform electrochemical measurements.

References

1. Panwar NL, Kaushik SC, Kothari S (2011) Role of renewable energy sources in environmental protection: a review. Renew Sustain Energy Rev 15:1513–1524. doi:10.1016/j.rser.2010.11.037
2. Ibrahim H, Ilinca A, Perron J (2008) Energy storage systems—characteristics and comparisons. Renew Sustain Energy Rev 12:1221–1250. doi:10.1016/j.rser.2007.01.023
3. Hall PJ, Bain EJ (2008) Energy-storage technologies and electricity generation. Energy Policy 36:4352–4355. doi:10.1016/j.enpol.2008.09.037
4. Wang G, Zhang L, Zhang J (2012) A review of electrode materials for electrochemical supercapacitors. Chem Soc Rev 41:797–828. doi:10.1039/c1cs15060j
5. Chandra A (2012) Supercapacitors: an alternate technology for energy storage. Proc Natl Acad Sci, India, Sect A 82:79–90. doi:10.1007/s40010-012-0009-9
6. Chandra A, Roberts AJ, Slade RCT (2008) Studies of nanostructures and conductivity in the system $V_xMo_{1-x}O_y$. Solid State Commun 147:83. doi:10.1016/j.ssc.2008.05.012
7. Arbizzani C, Mastragostino M, Soavi F (2001) New trends in electrochemical supercapacitors. J Power Sources 100:164–170. doi:10.1016/S0378-7753(01)00892-8
8. Zhang LL, Zhao XS (2009) Carbon-based materials as supercapacitor electrodes. Chem Soc Rev 38:2520–2531. doi:10.1039/b813846j
9. Chandra A, Roberts AJ, Yee ELH, Slade RCT (2009) Nanostructured oxides for energy storage applications in batteries and supercapacitors. Pure Appl Chem 81:1489–1498. doi:10.1351/PAC-CON-08-08-20
10. Frackowiak E, Beguin F (2001) Carbon materials for the electrochemical storage of energy in capacitors. Carbon 39:937–950. doi:S0008-6223(00)00183-4
11. Frackowiak E (2007) Carbon materials for supercapacitor application. Phys Chem Chem Phys 9:1774–1785. doi:10.1039/b618139m
12. Li L, Liu E, Li J, Yang Y, Shen H, Huang Z, Xiang X, Li W (2010) A doped activated carbon prepared from polyaniline for high performance supercapacitors. J Power Sources 195:1516–1521. doi:10.1016/j.jpowsour.2009.09.016
13. Rudge A, Davey J, Raistrick I, Gottesfeld S, Ferraris JP (1994) Conducting polymers as active materials in electrochemical capacitors. J Power Sources 47:89–107. doi:10.1016/0378-7753(94)80053-7
14. Lokhande CD, Dubal DP, Joo OS (2011) Metal oxide thin film based supercapacitors. Curr Appl Phys 11:1–16. doi:10.1016/j.cap.2010.12.001
15. Cross A, Morel A, Cormie A, Hollenkamp T, Donne S (2011) Enhanced manganese dioxide supercapacitor electrodes produced by electrodeposition. J Power Sources 196:7847–7853. doi:10.1016/j.jpowsour.2011.04.049
16. Ji X, Hallam PM, Houssein SM, Kadara R, Lang L, Banks CE (2012) Printable thin film supercapacitors utilizing single crystal cobalt hydroxide nanosheets. RSC Adv 2:1508–1515. doi:10.1039/c1ra01061a
17. Vivekchand SRC, Rout CS, Subrahmanyam KS, Govindaraj A, Rao CNR (2008) Graphene-based electrochemical supercapacitors. J Chem Sci 120:9–13. doi:10.1007/s12039-008-0002-7
18. Li Y, Zijll MV, Chiang S, Pan N (2011) KOH modified graphene nanosheets for supercapacitor electrodes. J Power Sources 196:6003–6006. doi:10.1016/j.jpowsour.2011.02.092
19. Jeong HK, Jin M, Ra EJ, Sheem KY, Han GH, Arepalli S, Lee YH (2010) Enhanced electric double layer capacitance of graphite oxide intercalated by poly(sodium 4-styrensulfonate) with high cycle stability. ACS Nano 4:1162–1166. doi:10.1021/nn901790f
20. Tien CP, Teng H (2010) Polymer/graphite oxide composites as high-performance materials for electric double layer capacitors. J Power Sources 195:2414–2418. doi:10.1016/j.jpowsour.2009.11.001
21. Wang J, Xu Y, Wang J, Du X (2011) Toward a high specific power and high stability polypyrrole supercapacitors. Synth Met 161:1141–1144. doi:10.1016/j.synthmet.2011.01.011
22. Peng XY, Liu XX, Diamond D, Lau KT (2011) Synthesis of electrochemically-reduced graphene oxide film with controllable size and thickness and its use in supercapacitor. Carbon 49:3488–3496. doi:10.1016/j.carbon.2011.04.047
23. Xing W, Huang CC, Zhuo SP, Yuan X, Wang GQ, Hulicova-Jurcakova D, Yan ZF, Lu GQ (2009) Hierarchical porous carbons with high performance for supercapacitor electrodes. Carbon 47:1715–1722. doi:10.1016/j.carbon.2009.02.024
24. Chen Y, Zhang X, Zhang H, Sun X, Zhang D, Ma Y (2012) High-performance supercapacitors based on a graphene-activated carbon composite prepared by chemical activation. RSC Adv 2:7747–7753. doi:10.1039/c2ra20667f
25. Marcano DC, Kosynkin DV, Berlin JM, Sinitskii A, Sun Z, Slesarev A, Alemany LB, Lu W, Tour JM (2010) Improved synthesis of graphene oxide. ACS Nano 4:4806–4814. doi:10.1021/nn1006368
26. Bissessur R, Liu PKY, Scully SF (2006) Intercalation of polypyrrole into graphite oxide. Synth Met 156:1023–1027. doi:10.1016/j.synthmet.2006.06.024
27. Kudin KN, Ozbas B, Schniepp HC, Prud'homme RK, Aksay IA, Car R (2007) Raman spectra of graphite oxide and functionalized graphene sheets. Nano Lett 8:36–41. doi:10.1021/nl071822y
28. Bose S, Kuila T, Uddin ME, Kim NH, Lau AKT, Lee JH (2010) In situ synthesis and characterization of electrically conductive polypyrrole/graphene nanocomposites. Polymer 51:5921–5928. doi:10.1016/j.polymer.2010.10.014
29. Yang S, Wu X, Chen C, Dong H, Hu W, Wang X (2012) Spherical α-$Ni(OH)_2$ nanoarchitecture grown on graphene as advanced electrochemical pseudocapacitor materials. Chem Commun 48:2773–2775. doi:10.1039/C2CC16565A
30. Gu Z, Zhang L, Li C (2009) Preparation of highly conductive polypyrrole/graphite oxide composites via in situ polymerization. J Macromol Sci B 48:1093–1102. doi:10.1080/00222340903035576
31. Demarconnay L, Raymundo-Pinero E, Beguin F (2010) A symmetric carbon/carbon supercapacitor operating at 1.6 V by using a neutral aqueous solution. Electrochem Commun 12:1275–1278. doi:10.1016/j.elecom.2010.06.036
32. Alvi F, Ram MK, Basnayaka PA, Stefanakos E, Goswami Y, Kumar A (2011) Graphene–polyethylenedioxythiophene conducting polymer nanocomposite based supercapacitor. Electrochim Acta 56:9406–9412. doi:10.1016/j.electacta.2011.08.024
33. Hashmi SA, Kumar A, Tripathi SK (2005) Investigations on electrochemical supercapacitors using polypyrrole redox electrodes and PMMA based gel electrolytes. Eur Polym J 41:1373–1379. doi:10.1016/j.eurpolymj.2004.12.013

34. Zhang D, Zhang X, Chen Y, Yu P, Wang C, Ma Y (2011) Enhanced capacitance and rate capability of graphene/polypyrrole composite as electrode material for supercapacitors. J Power Sources 196:5990–5996. doi:10.1016/j.jpowsour.2011.02.090
35. Davies A, Audette P, Farrow B, Hassan F, Chen Z, Choi JY, Yu A (2011) Graphene-based flexible supercapacitors: pulse-electropolymerization of polypyrrole on free-standing graphene films. J Phys Chem C115:17612–17620. doi:10.1021/jp205568v
36. Wang Y, Shi Z, Huang Y, Ma Y, Wang C, Chen M, Chen Y (2009) Supercapacitor devices based on graphene materials. J Phys Chem C 113:13103–13107. doi:10.1021/jp902214f
37. Wang J, Xu Y, Zhu J, Ren P (2012) Electrochemical in situ polymerization of reduced graphene oxide/polypyrrole composite with high power density. J Power Sources 208:138–143. doi:10.1016/j.jpowsour.2012.02.018
38. Wang W, Hao Q, Lei W, Xia X, Wang X (2012) Graphene/SnO_2/polypyrrole ternary nanocomposites as supercapacitor electrode materials. RSC Adv 2:10268–10274. doi:10.1039/C2RA21292G